

The Role of Iodanyl Radicals as Critical Chain Carriers in Aerobic Hypervalent Iodine Chemistry

Sung-Min Hyun,[†] Mingbin Yuan,[§] Asim Maity,[†] Osvaldo Gutierrez,^{§,*} David C. Powers^{†,*}

[†] Department of Chemistry, Texas A&M University, College Station, Texas 77843, United States

[§] Department of Chemistry and Biochemistry, University of Maryland, College Park, Maryland 20742, United States

Summary Selective O₂ utilization remains a substantial challenge in synthetic chemistry. Biological small-molecule oxidation reactions often utilize aerobically generated high-valent catalyst intermediates to effect substrate oxidation. Available synthetic methods for aerobic oxidation catalysis are largely limited to substrate functionalization chemistry by low-valent catalyst intermediates (*i.e.* aerobically generated Pd(II) intermediates). Motivated by the need for new chemical platforms for aerobic oxidation catalysis, we have recently developed aerobic hypervalent iodine chemistry. Here, we report that in contrast to canonical two-electron oxidation mechanisms for the oxidation of organoiodides, the developed aerobic hypervalent iodine chemistry proceeds via a radical chain mechanism initiated by addition of aerobically generated acetoxy radicals to aryl iodides. Despite the radical chain mechanism, aerobic hypervalent iodine chemistry displays similar substrate tolerance observed with traditional terminal oxidants, such as peracids. We anticipate these insights will enable new sustainable oxidation chemistry via hypervalent iodine intermediates.

Bigger Picture O₂ is routinely utilized in biological catalysis to generate high-valent catalyst intermediates that engage in substrate oxidation chemistry. Analogous synthetic chemistry via aerobically generated high-valent intermediates would enable new sustainable synthetic methods, but due to challenges in selective O₂ utilization, is largely unknown. We have developed aerobic hypervalent iodine chemistry as a platform to couple O₂ reduction with a diverse set of substrate functionalization mechanisms. Many of the synthetic applications of hypervalent iodine reagents rely on selective two-electron oxidation-reduction chemistry. Here we report that one-electron oxidation reactions pathways via iodanyl radical intermediates are critical in aerobic hypervalent iodine chemistry. The new appreciation for the critical role iodanyl radicals can play in the synthesis of hypervalent iodine compounds will provide new opportunities in sustainable oxidation catalysis.

Introduction

O_2 is an attractive oxidant for use in synthetic chemistry because it is readily available, generates environmentally benign byproducts, and displays substantial reduction potential. Radical chain autoxidation—the spontaneous oxidation of organic compounds upon exposure to O_2 —is a ubiquitous process in organic chemistry that can affect most organic functional groups.¹⁻⁴ Autoxidation chain reactions arise due to spin conservative reactions of the triplet ground state of O_2 (*i.e.* ${}^3\text{O}_2$) with singlet organic molecules. On commodity scale, autoxidation of cumene and *p*-xylene produce phenol⁵ and terephthalic acid,⁶ respectively (Figure 1b). In fine-chemical synthesis, acyl radical intermediates generated during aldehyde autoxidation (Figure 2a) have been diverted towards olefin addition chemistry (Figure 2b),⁷⁻⁸ alkyl radical intermediates generated by decarbonylation of acyl radicals have been harnessed for alkylation of *N*-heterocycle (Figure 2c),⁹ and peroxy radicals and peroxide intermediates have been diverted towards oxygen-atom transfer (OAT) chemistry to olefins (*i.e.* Mukaiyama reaction)¹⁰⁻¹² ¹⁰⁻¹⁵ ¹⁰⁻¹⁵ and to transition metal complexes (Figure 2d and Figure 2e).¹³⁻¹⁵ While these examples highlight the potential of autoxidation in specific synthetic applications, reliance on only those reactive intermediates generated in autoxidation chemistry substantially limits the diversity of substrate functionalization reactions that can be coupled to O_2 .

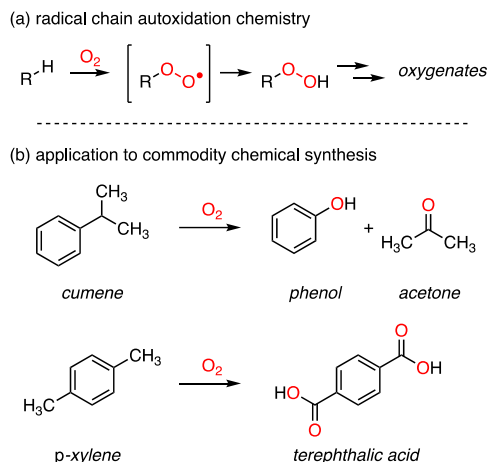


Figure 1. (a) Autoxidation reactions proceed via peroxy radical and hydroperoxide intermediates. (b) Autoxidation chemistry is utilized on commodity scale to produce phenol, acetone, and terephthalic acid.

Motivated by the desire to couple diverse substrate oxidation mechanisms to the reduction of O_2 , a wide variety of aerobic oxidation methods have been developed. Among the most well-developed is Pd oxidase chemistry, in which the diverse substrate functionalization mechanisms available to Pd(II) are coupled to aerobic re-oxidation of Pd(0) intermediates in catalysis.¹⁶⁻²¹ Pd oxidase chemistry has been leveraged for a wide variety of substrate functionalization reactions — alcohol²²⁻²⁴ and olefin oxidation, Aza-Wacker chemistry,²⁵ arene oxidation,²⁶⁻²⁷ oxidative Heck reactions,²⁸⁻³¹ and allylic oxidation³²⁻³³ — however, from a mechanistic perspective, available methods are limited to those which can be achieved by low-valent Pd catalysis (*i.e.* Pd(0)/Pd(II) cycles). General strategies that access to high oxidation state catalytic cycles with O_2 are largely unavailable.³⁴⁻³⁹

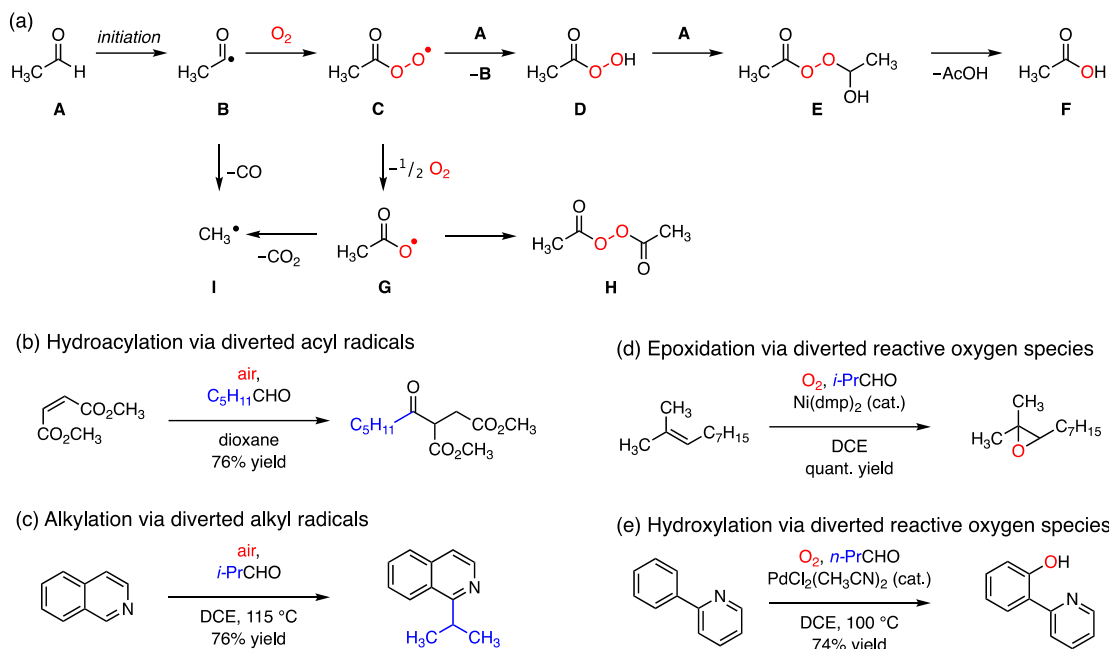


Figure 2. (a) The manifold of reaction chemistry that is available during the autoxidation of acetaldehyde. Reactive intermediates in aldehyde autoxidation have been redirected in order to accomplish (b) olefin addition chemistry, (c) alkylation reactions, (d) oxygen-atom transfer (OAT), and (e) transition-metal-catalyzed hydroxylation.

In the absence of aerobically generated two-electron oxidants capable of mediating substrate functionalization chemistry via high-valent intermediates, an array of designer synthetic oxidants has been developed. Hypervalent iodine compounds have emerged as a particularly useful class of reagents that find application in mechanistically diverse oxidation reactions including α -oxidation of carbonyl compounds, alcohol and amine dehydrogenations, oxidative dearomatization chemistry, olefin functionalization, group transfer chemistry, and transition metal catalysis.⁴⁰⁻⁴⁷ The utility of these reagents derives from (1) the substantial reduction potential of many of these reagents, (2) the often-observed two-electron oxidation-reduction chemistry,⁴⁷⁻⁵⁷ and (3) the facility of ligand exchange reactions at hypervalent iodine centers. Drawbacks of hypervalent iodine reagents include common requirement for (super)stoichiometric loading of these reagents and the generation of substantial chemical waste, during both preparation and utilization of these species. If aerobic hypervalent iodine chemistry were realized as a general platform, it would be complementary to existing methodologies by providing entry to high oxidation state catalytic cycles with O_2 .

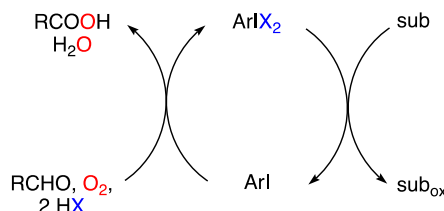


Figure 3. Aerobically generated hypervalent iodine intermediates present a strategy to accomplishing aerobic oxidation catalysis via strongly oxidizing intermediates.

In 2018, we demonstrated that the aerobic synthesis of hypervalent iodine reagents could be accomplished by diverting reactive aldehyde-autoxidation intermediates and that the aerobically generated hypervalent iodine species can be utilized as intermediates in a variety of synthetic chemistry (Figure 3).⁵⁸⁻⁶⁰ This approach couples strongly oxidizing intermediates generated during aldehyde autoxidation with disparate substrate oxidation mechanisms. This strategy has provided a platform to couple O₂ reduction with the broad classes of substrate functionalization chemistry that is available to hypervalent iodine reagents, such as α -carbonyl oxidation, oxidative dearomative cyclization, C–H / N–H coupling and alcohol dehydrogenation chemistry. Based on the frequency with which peracids are used in the synthesis of hypervalent iodine reagents,⁶¹⁻⁶⁵ our initial investigations were predicated on the hypothesis that aerobically generated peracetic acid **D** could be diverted towards the oxidation of PhI. Here, we report a detailed experimental and theoretical investigation of aldehyde-promoted oxidation of aryl iodides. A combination of *in situ* spectroscopy, kinetic studies, and computational investigations support a mechanism in which aldehyde-promoted aerobic oxidation of aryl iodides proceeds via one-electron oxidation at iodine to generate iodanyl radicals, which subsequently generate the observed I(III) products via a radical chain mechanism. The results of these studies provide evidence for the critical role of single-electron chemistry and open-shell intermediates in hypervalent iodine chemistry, and substantially enriches the mechanistic landscape available for the synthesis of these important reagents.

Results

Figure 2a illustrates the manifold of reactions operative during the autoxidation of acetaldehyde.⁶⁶⁻⁶⁷ Hydrogen-atom abstraction (HAA) from acetaldehyde **A** generates acyl radical **B**, which rapidly reacts with O₂ to generate peroxy radical **C**.⁶⁸ HAA from a second equivalent of acetaldehyde affords radical chain carrier **B** and an equivalent of peracetic acid **D**. Baeyer–Villiger reaction of **D** with **A** affords acetic acid via the intermediacy of peroxide **E**. In addition, dimerization of peroxy radical **C** generates ¹O₂ and two equivalents of acetoxy radical **G** via the fragmentation of a transient tetroxide intermediate (*i.e.* Russell termination).⁶⁹⁻⁷³ Dimerization of acetoxy radicals **G** generates diacetyl peroxide **H**.⁶⁶ Methyl radicals **I** can arise by decarboxylation of **G** or by decarbonylation of **B**.⁶⁶⁻⁶⁷ A number of the species illustrated in Figure 2a—oxygen-centered radicals **C** and **G**, peroxides **E** and **H**, and peracetic acid—are potential oxidants of aryl iodides during aldehyde-promoted aerobic oxidation.

Identification of Potential Oxidants. Previously, we observed initial formation and subsequent consumption of peroxide **E** during acetaldehyde-promoted oxidation of iodobenzene (PhI) by *in situ* ¹H NMR spectroscopy.⁵⁸ A ¹H NMR magnetization transfer experiment demonstrated that **E** equilibrates with acetaldehyde and peracetic acid rapidly relative to PhI oxidation. To evaluate the presence of open-shell intermediates during the aerobic oxidation of PhI, we have carried out a series of EPR measurements using *N*-*tert*-butyl- α -phenylnitron (PBN, **1**), as a radical spin trap (Figure 4).⁷⁴ Figure 4a illustrates the X-band EPR spectrum obtained following addition of PBN to the reaction mixture of PhI, acetaldehyde, O₂, and CoCl₂. The spectrum can be fit as the admixture of a triplet of doublets ($a_H = 2.14$ G, $a_N = 14.06$ G) and a triplet ($a_N = 7.86$ G). The triplet of doublets is attributed to PBN-trapped acetoxy radical (**2**; Figure 4b)⁷⁵⁻⁷⁶ and the triplet is attributed to a radical arising from single-electron oxidation of PBN (**3**, Figure 4c).⁷⁷ The formation of PBN-trapped acetoxy radical **2** was confirmed by electrospray

ionization-mass spectrometry (ESI-MS) analysis ($m/z = 258.1100$, $[\text{M}+\text{Na}]^+$; Figure S1). Addition of PBN to the acetaldehyde-promoted oxidation of PhI in 1,2-dichloroethane (DCE) and CH_2Cl_2 also displays spectral features arising from compounds **2** and **3** (Figure S2). The presence of open-shell intermediates was further implicated by analysis of the headspace of a reaction in which PhI is oxidized under the dual action of acetaldehyde and O_2 , which revealed that in addition to acetaldehyde, trace CO_2 and CO were observed (Figure S3). These observations implicate the generation of acyl radical intermediates during aldehyde autoxidation.

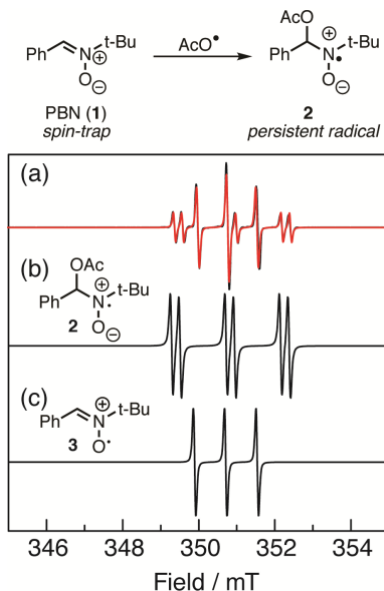


Figure 4. (a) X-band EPR spectrum obtained following addition of PBN (**1**) to the oxidation of PhI in AcOH; experimental data (black trace), fitting (red trace). The obtained spectrum displays features of both **2** and **3**. (b) Simulated spectrum of acetoxy radical adduct **2**. (c) Simulated spectrum of one-electron oxidation product **3**.

Evaluation of the Oxidation of PhI by Potential Closed-Shell Oxidants. We have pursued the following experiments to evaluate the chemical competence of peracetic acid, Baeyer-Villiger peroxide **E**, diacetyl peroxide, and $\text{Co}(\text{OAc})_3$ as primary oxidants in the aldehyde-promoted aerobic oxidation of aryl iodides.

Peracetic Acid. Peracetic acid **D** is often employed as the terminal oxidant in the synthesis of hypervalent iodine reagents. In our hands, treatment of PhI with a commercially obtained 32 wt% peracetic acid (5 equiv) in AcOH affords $\text{PhI}(\text{OAc})_2$ in 92% yield, which confirms the chemical competence of peracetic acid as an oxidant of PhI.

Baeyer-Villiger Peroxides. Addition of a commercially available solution of peracetic acid to acetaldehyde results in the evolution of peroxide **E**,⁷⁸ along with 1-hydroperoxyethan-1-ol, the adduct of H_2O_2 and acetaldehyde (Figure S4). Exposure of PhI to reaction mixtures containing peroxide **E** resulted in no $\text{PhI}(\text{OAc})_2$ after 13 h (Figure S5), which indicates that peroxide **E** is not a competent oxidant of PhI.

Diacetyl Peroxide. Diacetyl peroxide is potentially generated during acetaldehyde autoxidation by dimerization of acetoxy radicals.⁶⁶ Treatment of PhI with independently synthesized⁷⁹ diacetyl peroxide **H** in $\text{AcOH-}d_4$ at 23 °C resulted in no reaction as ascertained by ^1H

NMR analysis for 17 h (Figure S6–S9). A potassium iodide (KI) test confirmed presence of peroxide after the reaction.

Co(OAc)_3 . To insure consistent initiation of aldehyde autoxidation,^{80–81} Co(II) salts are included in the optimized conditions for aldehyde-promoted PhI. In addition to functioning as an autoxidation initiator, Co(III) species can oxidize peracids to generate peroxy radicals (*i.e.* oxidation of **D** to generate **C**) and Co(II) species are readily oxidized to Co(III) by peracids (*i.e.* **D**).⁸² One might also envision direct oxidation of PhI by Co(III).^{82–83} The following lines of experimental evidence suggest that Co-based additives are not intimately involved in the oxidation of PhI: (1) Co-based promoters are not necessary for aldehyde-promoted aerobic oxidation of aryl iodide. Removal of these additives from aerobic oxidation reactions results in variable initiation time but a high yield of PhI(OAc)_2 can still be obtained.⁵⁸ (2) Exposure of PhI to an AcOH solution of Co(OAc)_3 ⁸², which is the product of aerobic oxidation of Co(II) in AcOH, did not result in the observation of any PhI(OAc)_2 (Figure S10). (3) Comparison of the concentration versus time plots for aerobic oxidation with and without Co(II) (1 mol% $\text{CoCl}_2 \cdot 6\text{H}_2\text{O}$; Figure S11) reveals that while the length of time that is required for initiation depends intimately on the presence of Co(II), once oxidation commences the presence of Co initiators does not impact the kinetics of oxidation.

Hammett Analysis. To probe the nature of the kinetically relevant oxidants responsible for aldehyde-promoted aerobic oxidation of aryl iodides, we have evaluated the impact of aryl iodide substitution on the rate of aryl iodide oxidation for both aldehyde-promoted aerobic oxidation and peracetic acid mediated protocols (Figure 5). Due to the presence of a kinetic induction period during aldehyde-promoted aerobic oxidation of aryl iodides, initial rate data was obtained with a series of competition experiments in which pairs of aryl iodides were exposed to aldehyde-promoted aerobic oxidation conditions (Figure 5a; see Figures S12–S14 and Table S1–S2 for raw data).⁸⁴ Each competition reaction was carried out in triplicate. The resulting data for aldehyde-promoted oxidation of aryl iodides is well-correlated with σ^+ parameters ($\rho = -0.51$, $R^2 = 0.98$; Figure 5a) and less-well correlated with σ parameters ($R^2 = 0.93$; Figure S15). In contrast, the Hammett plot pictured in Figure 5b, which displays the initial rate data for peracetic acid oxidation of aryl iodides, is well-correlated with both σ parameters ($\rho = -2.10$, $R^2 = 0.93$; Figure 5b see Figures S16 and Table S3–S4 for raw data) and is less-well correlated with σ^+ parameters ($R^2 = 0.85$; Figure S17).⁸⁵ The significantly different slopes of the Hammett plots pictured in Figure 5 indicate that aldehyde-promoted aerobic oxidation and peracid-mediated oxidation do not proceed via the same rate-determining transition state.

The sensitivity of aldehyde-promoted oxidation ($\rho = -0.51$) indicates the buildup of positive charge during the rate-determining transition state of aldehyde-promoted aerobic oxidation, but substantially less than is observed during peracid oxidation ($\rho = -2.10$). The ρ -value for aldehyde-promoted oxidation is similar to ρ -values that have been reported for the radical autoxidation of cumene derivatives ($\rho = -0.41$)⁸⁶ and for the epoxidation of stilbene derivatives under aldehyde-autoxidation conditions ($\rho = -0.73$)⁸⁷ (a reaction proposed to proceed via initial addition of an aerobically generated acyl peroxy radical to the olefin). These results 1) demonstrate that peracetic acid is not kinetically competent as the oxidant during aldehyde-promoted aerobic

oxidation and 2) suggest that open-shell species may serve as critical oxidants during aldehyde-promoted aerobic oxidation.

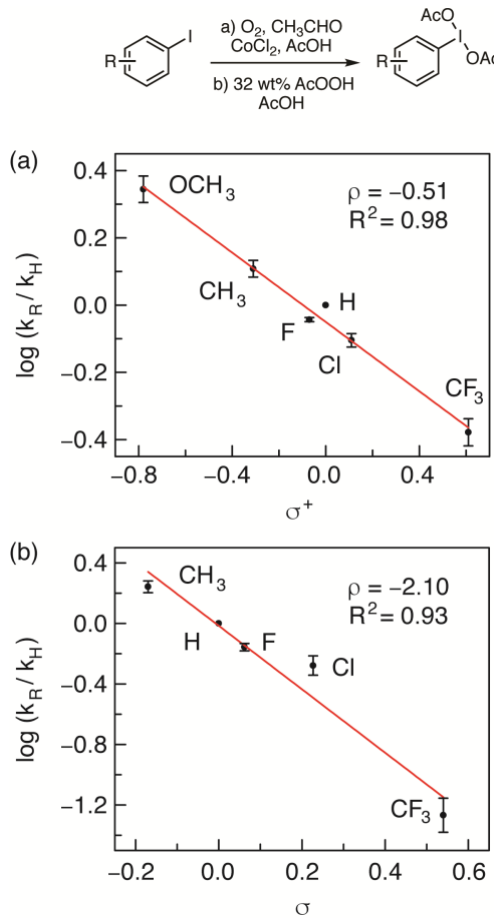


Figure 5. Hammett plots of (a) the aldehyde-promoted aerobic oxidation of aryl iodides and (b) the peracetic acid oxidation of aryl iodides.

Evaluation of the Oxidation of PhI by Potential Open-Shell Oxidants. Based on the observation of oxygen-centered radicals by spin-trapped EPR and the results of Hammett analysis, we have pursued a series of experiments to evaluate the competence of these species as oxidants for PhI.

Kinetic Competition Experiments. Reactive oxidants generated during the autoxidation of aldehydes have previously been demonstrated to be competent oxidants towards aliphatic C–H bonds.^{88–89} In our hands, exposure of a solution of cyclohexane and acetaldehyde to O₂ afforded cyclohexanone in 9.5% yield (Table 1, Entry 1). Using a mixture of d₁₂- and H₁₂-cyclohexane, we measured the kinetic isotope effect (KIE) for cyclohexane oxidation under these conditions to be 4.8(4), which suggests that HAA from cyclohexane is the rate determining step in the generation of cyclohexanone. Using dispersion-corrected DFT (UB3LYP-D3/def2-TZVPP-SMD(DCE)), we have identified the barriers for HAA from cyclohexane by acetoxy radical **G** to be 10.8 kcal/mol (computed $k_H/k_D = 3.6$) and by peroxy radical **C** to be 17.3 kcal/mol (computed $k_H/k_D = 6.1$) (Figure S18). Previous measurements of the kinetic isotope effects for HAA by peroxy radicals have reported large values ($k_H/k_D = 9–19$).^{71, 86, 90} The observation of acetoxy radicals by PBN-trapped EPR spectroscopy, in combination with the measured kinetic isotope effect suggests that

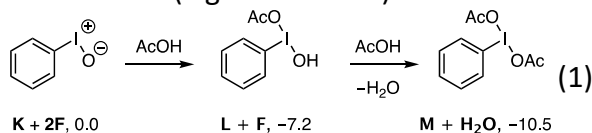
cyclohexane oxidation most likely proceeds via initial HAA from cyclohexane by acetoxy radical **G**.

To evaluate the kinetic competence of acetoxy radical **G** for oxidation of PhI, we examined the aldehyde promoted oxidation of hydrocarbon substrates in the presence of added PhI. We reasoned that if the reactive oxygen-centered radicals responsible for C–H oxidation of cyclohexane (*i.e.* **G**) were also responsible for PhI oxidation, PhI would be a competitive inhibitor of cyclohexane oxidation. Consistent with this hypothesis, addition of an increasing amount of PhI to aldehyde-promoted cyclohexane oxidation reactions resulted in the suppression of cyclohexanone evolution (Table 1, Entries 2–4). Similarly, exposure of adamantane to acetaldehyde autoxidation reaction mixtures results in 1-adamantanol in 47% yield,⁹¹ which is reduced to 14% upon the addition of 1.0 equivalents of PhI, and exposure of ethylbenzene to acetaldehyde autoxidation reaction mixtures results in acetophenone in 30% yield, which is reduced to 9% upon addition of PhI. The yields for C–H oxidation and iodobenzene oxidation are anti-correlated: For example, during oxidation of ethylbenzene, in the presence of 1.0 equivalent of PhI, acetophenone is generated in 9% yield and PhI(OAc)₂ is generated in 53% yield; in the presence of 5.0 equivalent of PhI, acetophenone is generated in 5% yield and PhI(OAc)₂ is generated in 100% yield (based on ethylbenzene). These data indicate that PhI is a kinetic inhibitor of C–H oxidation and thus implicates open-shell oxidants in the oxidation of PhI (Table S5–S7).

Table 1. Products from the addition of PhI to aldehyde autoxidation reactions in the presence of cyclohexane.

entry	PhI loading	cyclohexanone yield (%)
1	0.00 equiv	9.5
2	1.00 equiv	2.4
3	5.00 equiv	2.0
4	10.0 equiv	0.8

Computational Results In this section, we evaluate pathways that would generate either iodosylbenzene (**K**)⁹² or (diacetoxyiodo)benzene (**M**) because under the reaction conditions we have examined (*i.e.* in the presence of AcOH), iodosylbenzene is readily converted to (diacetoxyiodo)benzene via the intermediacy of hydroxy iodinane **L** (Eqn 1).⁹³ See Supporting Information for computational details (Figure S19–S29).



Pathways via Initial Two-Electron Oxidation. We initiated our computational investigation by evaluating potential two-electron OAT reactions from peracetic acid, peroxy radical **C**, and acetoxy radical **G** to afford iodosylbenzene (Figure 6).⁹⁴ The lowest energy transition state located

for oxygenation of PhI by peracetic acid is **TS_{DJ-FK}** (22.2 kcal/mol vs. PhI and **D**) in which OAT is activated by internal hydrogen bonding of the peracid proton to the carbonyl group (Figure 6a). The located transition state is analogous to the butterfly transition states invoked for olefin epoxidation with peracids.⁹⁵ Potential ionic mechanisms via initial hydroxylation of PhI followed by recombination with acetate anions were not found to be lower in energy (Figure S21). We have also evaluated OAT from peroxy radical **C** and acetoxy radical **G**, reaction steps that have been suggested to be operative in the autoxidation of phosphorous(III) compounds.⁹⁶⁻¹⁰² Both processes are substantially endergonic — OAT from **C** to generate iodosylbenzene **K** and acetoxy radical **G** is +12.1 kcal/mol and OAT from **G** to generate iodosylbenzene **K** and acyl radical **B** is +67.3 kcal/mol — and thus we will not consider these pathways further.

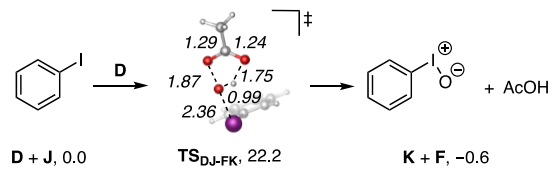


Figure 6. Evaluation of OAT from peracetic acid to PhI. Free energies (kcal/mol) were computed at the UB3LYP-D3/def2-TZVPP-SMD(DCE) level of theory.

Pathways via Initial One-Electron Oxidation. Based on Hammett analyses and PhI-mediated inhibition of C–H oxidation chemistry, we have examined one-electron oxidation pathways for the reaction of reactive intermediates generated during aldehyde autoxidation (e.g. acetoxy radical **G**) with PhI.¹⁰³ Addition of acetoxy radical to form iodanyl radical **N** is uphill by 3.9 kcal/mol and is accessed via **TS_{GJ-N}**, which is 8.9 kcal/mol above the separated reactants (Figure 7). Iodanyl radical **N** displays a bent geometry at the hypervalent iodine center (C–I–O: 97.6°) and a long I–O bond (2.63 Å; for comparison I–O in **M**: 2.19 Å (computed); 2.16 (expt)¹⁰⁴). Iodanyl radical **N** resembles intermediates proposed during alkynylation reactions accomplished by photoredox catalysis.¹⁰⁵⁻¹⁰⁶ Evaluation of the spin density of **N** indicates that substantial spin on the iodine center with delocalization to the oxygen atoms of the acetate ligand (see Table S8 for detailed analysis of the spin density of **N**). An I(II) compound resulting from addition of peroxy radical **C** to PhI could not be located as a stationary point; all attempts resulted in evolution of iodosylbenzene with extrusion of acetoxy radical as depicted in Figure 6.

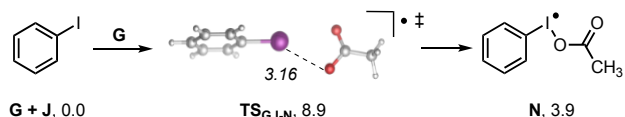


Figure 7. Computed pathways for initiation steps in which oxygen-centered radicals are added to PhI. Free energies (kcal/mol) were computed at the UB3LYP-D3/def2-TZVPP-SMD(DCE) level of theory.

Reaction of I(II) intermediates (*i.e.* **N**) with peroxides present in solution would result in radical chain propagation. Based on the relative facility of acetoxy versus peroxy radical addition to PhI, we have evaluated a variety of potential reaction pathways for reactions of iodanyl radical **N** (Figure 8). Addition of peracetic acid to iodanyl radical **N** to generate hydroxy iodonane **L** and acetoxy radical is downhill by 11.7 kcal/mol and proceeds via transition state **TS_{DN-GL}**, which is calculated to be 17.2 kcal/mol above the separated reactants. Similarly, reaction of iodanyl

radical **N** with either diacetyl peroxide **H** or peroxide **E** to generate I(III) products and generate chain-carrying acetoxy radicals are both thermodynamically favored and proceed via transition states of similar, yet higher, energy (Figure S25). Chain-propagating addition of peracetic acid to iodanyl radical **N** is the highest barrier along the computed pathway from PhI to PhI(OAc)_2 ¹⁰⁷ and computational evaluation of the impact of substituents on the barrier of this step is consistent with the experimentally defined Hammett relationship featured in Figure 5a (see Figures S26 and S27 for details).

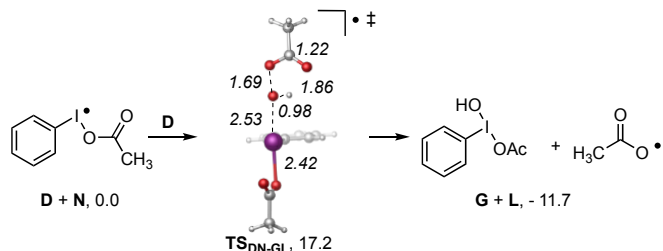


Figure 8. Computed pathways for radical chain propagation by reaction of iodanyl radical **N** with peracetic acid **D**. Free energies (kcal/mol) were computed at the UB3LYP-D3/def2-TZVPP-SMD(DCE) level of theory.

Reaction of transiently generated iodanyl radicals with open-shell species in solution would result in chain termination. We considered several potential termination pathways (Figure 9). Disproportionation of two equivalents of iodanyl radical **N** to generate (diacetoxyiodo)benzene and iodobenzene is thermodynamically favored (-30.3 kcal/mol); we have been unable to locate a transition state for this process (Figure 9a). The addition of acetoxy radical **G** to iodanyl radical **N** proceeds without barrier (Figure 9b), as determined by scan about the O–I bond, leading to (diacetoxyiodo)benzene (-26.4 kcal/mol). In addition to productive termination steps leading to the production of PhI(OAc)_2 , unproductive termination, such as loss of acetoxy radical followed by radical coupling to generate diacetyl peroxide is also downhill (Figure 9c).

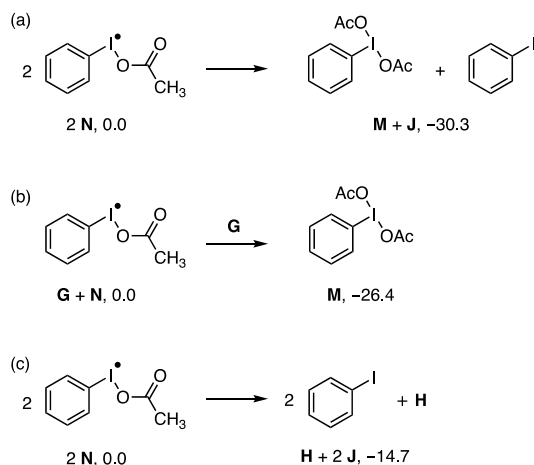


Figure 9. Reaction pathways for (a) disproportionation of two equivalents of iodanyl radical **N**, (b) addition of acetoxy radical **G** to iodanyl radical **N**, and (c) loss of diacyl peroxide **H** from two equivalents of iodanyl radical **N**. Free energies (kcal/mol) were computed at the UB3LYP-D3/def2-TZVPP-SMD(DCE) level of theory.

Summary of Mechanistic Data. Figure 10 summarizes the radical chain process that is consistent with the available experimental and computational results. Addition of acetoxy radical

G to **PhI** generates iodanyl radical **N**. Reaction of **N** with peracetic acid generates hydroxy iodonane **L**, which reacts spontaneously with **AcOH** to afford the observed **PhI(OAc)₂**, and regenerates acetoxy radical **G**. Radical chain termination is accomplished by either combination of iodanyl radical **N** with acetoxy radical **G** or by disproportionation of iodanyl radical **N**. In this chain reaction, both iodanyl radical **N** and acetoxy radical **G** are chain carriers. The oxidation mechanism that has emerged from these studies shares common features with autoxidation reactions of some main-group species and transition metal complexes, which—unlike simple organics—can access expanded valences. For example, the radical autoxidation of phosphorous(III) derivatives to generate phosphorous(V) oxides has been extensively studied (Figure 11b).⁹⁶⁻¹⁰² Based on both kinetic data and EPR spectroscopy, four-coordinate phosphanyl radicals, generated by the addition of peroxy and alkoxy radicals to P(III) derivatives, have been implicated as autoxidation intermediates. Similarly, during the aerobic oxidation of dimethyl Pd(II) complexes, transient peroxy Pd(III) intermediates generated by addition of oxygen-centered radicals have been implicated (Figure 11c).¹⁰⁸

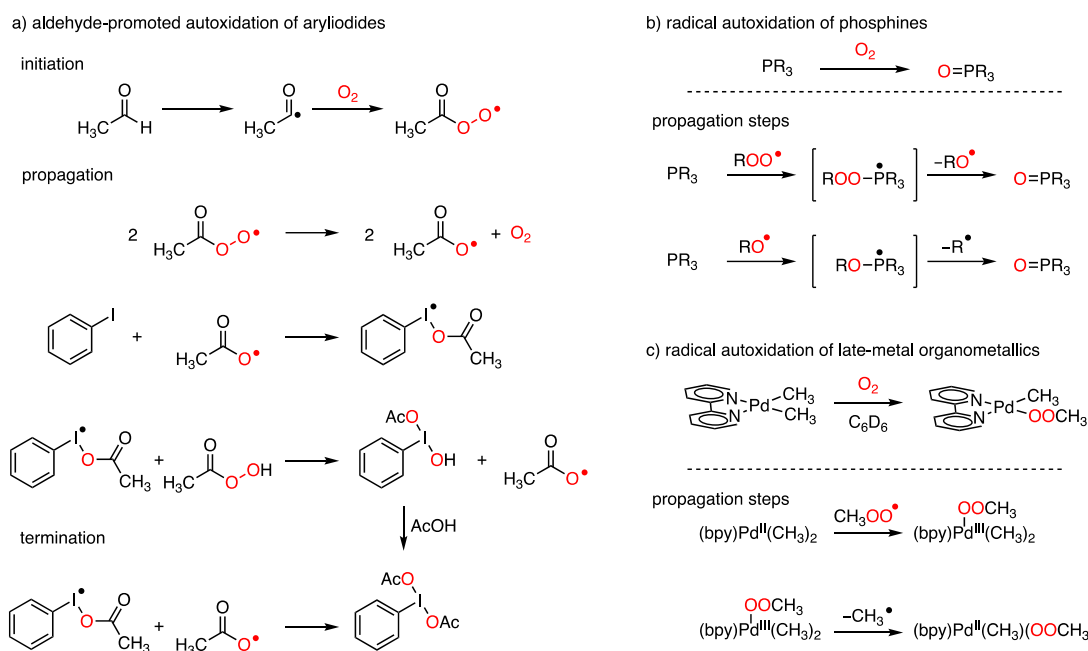


Figure 10. (a) Summary of the reaction steps involved in aldehyde-promoted aerobic oxidation of aryl iodides. Valence expansion during radical chain autoxidation has also been implicated during (b) the autoxidation of P(III) compounds and (c) the autoxidation of late-metal complexes.

Analysis of the free energy surface for two-electron oxidation of **PhI** by peracetic acid versus the radical chain mechanism advanced for aldehyde-promoted aerobic oxidation rationalizes the observation that while peracetic acid is a chemically competent oxidant for **PhI**, it is not kinetically competent during aldehyde-promoted aerobic oxidation. Addition of acetoxy radical to **PhI** proceeds with a barrier of 8.9 kcal/mol. The barrier to oxidation of **PhI** by peracetic acid is computed to be 22.2 kcal/mol while the highest barrier calculated along the radical chain mechanism depicted in Figure 10 is oxidation of iodanyl radical **N** by peracetic acid at 21.1 kcal/mol. These relative barrier heights are consistent with a Curtin-Hammett scenario, in which

rapid reversible addition of acetoxy radical to PhI proceeds to generate **N**, and selectivity for one-versus two-electron oxidation is governed by the relative barrier heights for reaction of peracetic acid with **N** and PhI, respectively.

Impact on Synthetic Chemistry. Interest in understanding the mechanism(s) relevant to aerobic hypervalent iodine chemistry is in part motivated by desire to enable aerobic oxidation catalysis via hypervalent iodine intermediates. A serious challenge to achieving hypervalent iodine catalysis is the relative rates of iodine-centered oxidation and direct substrate oxidation by the terminal oxidant. Substantial recent progress has been made towards realizing hypervalent iodine catalysis using mCPBA and other peracids as terminal oxidants. To evaluate the functional group tolerance of the radical chain aerobic oxidation of PhI, we have carried out robustness analyses¹⁰⁹ for PhI oxidation by both our aerobic protocol and for mCPBA oxidation (Figure 11). In this experiment, small-molecule featuring a variety of functional groups are added to a reaction and both the impact on the reaction yield and the amount of recovered additive are recorded. The results of these experiments reveal that despite the radical chain mechanism, the functional group tolerance of the two conditions is remarkably similar. Challenges to both sets of conditions include electron rich aromatic substrates (*i.e.* phenol and aniline) and C–C multiply bonded substrates. Similar analysis of the aryliodide catalyzed cross-coupling of benzene with *N*-methoxy-4-methylbenzenesulfonamide is detailed in the Supporting Information.

Robustness Analysis for PhI Oxidation

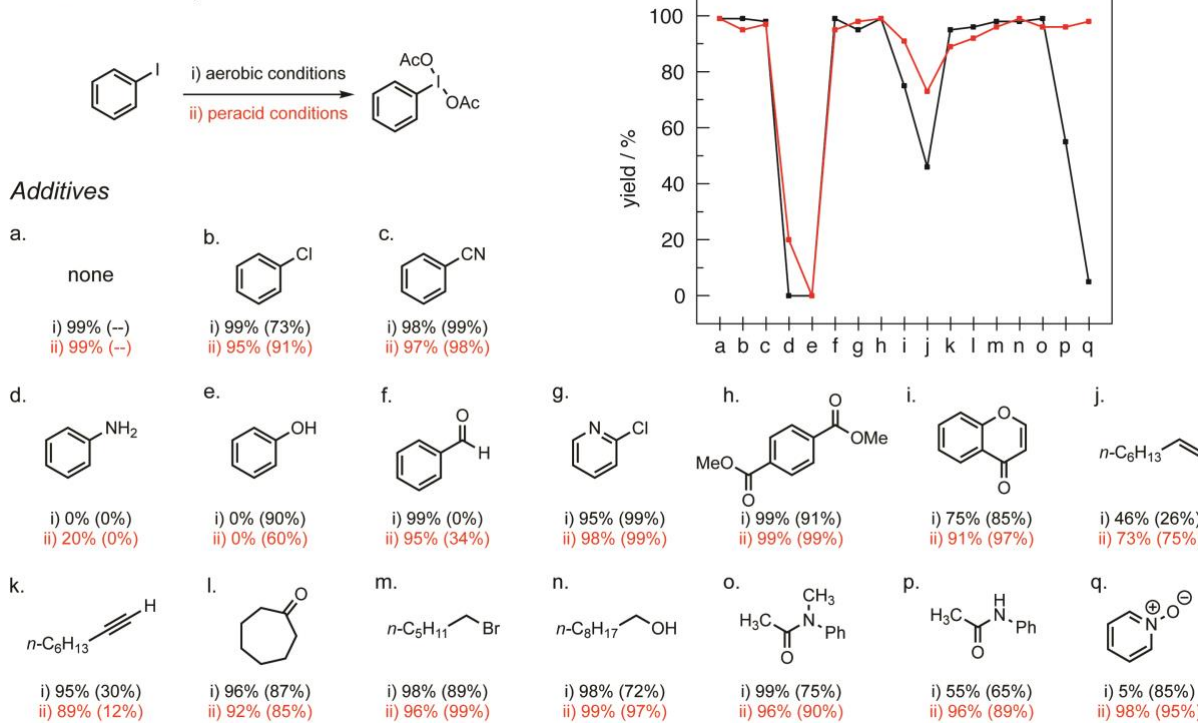


Figure 11. Robustness analysis for aerobic oxidation of PhI. The functional group tolerance for aerobic oxidation (black) is similar to that of mCPBA oxidation (red).

Conclusions

Development of new strategies to couple O_2 reduction with oxidative substrate functionalization chemistry is required in order to realize sustainable synthetic chemistry. In

furtherance of this goal, we have developed new strategies to access hypervalent iodine compounds from O_2 by intercepting reactive oxidants generated during aldehyde autoxidation chemistry. Here we utilize experiment and theory to demonstrate that hypervalent iodine reagents are accessed by a radical chain reaction initiated by aerobically generated acetoxy radicals. Aerobically generated acetoxy radicals and the iodanyl radicals resulting from their addition to aryl iodides are critical chain-carriers during aerobic oxidation. This report represents the first demonstration of the important role of I(II) species during the oxidation of aryl iodides. These observations are striking given that application of hypervalent iodine reagents in synthesis is largely predicated on the well-behaved two-electron oxidation-reduction chemistry characteristic of these species.

A continuing challenge for the development of sustainable oxidation chemistry is the need to identify chemical strategies that provide access to strong chemical oxidants, such as hypervalent iodine compounds, under sufficiently mild conditions to be compatible with broad families of substrates. Robustness analysis reveals that the developed aerobic oxidation chemistry displays similar substrate tolerance to more commonly employed peracid-based methods, but oxidatively labile substrates, such as olefins, remain a challenge. We anticipate that the demonstration of the critical role of one-electron processes and iodanyl radical intermediates in the preparation of hypervalent iodine reagents will provide the mechanistic basis for the development of strategies to achieve sustainable substrate oxidation under mild reaction conditions.

ACKNOWLEDGMENT

The authors thank Texas A&M University, the University of Maryland College Park, the Welch Foundation grant A-1907 (to D.C.P.), and the National Science Foundation (CAREER 1751568 (to O.G.) and CAREER 1848135) for financial support, the UMD Deepthought2, MARCC/BlueCrab HPC, and XSEDE (CHE160082 and CHE160053) for computational resources, and Siyoung Sung for assistance with GC measurements.

AUTHOR CONTRIBUTIONS

OG and DCP designed the study. SMH and AM carried out experimental work and MY carried out computational studies. All authors contributed to interpreting the data and writing the manuscript.

COMPETING INTERESTS

The authors declare no competing interests.

REFERENCES

1. Howard, J. A. (1973). *Homogeneous Liquid Phase Autoxidations in Free Radicals* (John Wiley & Sons).
2. Walling, C. (1995). *Autoxidation* (Blackie Academic and Professional).
3. Lucarini, M., and Pedulli, G. F. (2010). Free Radical Intermediates in the Inhibition of the Autoxidation Reaction. *Chem. Soc. Rev.* **39**, 2106–2119.
4. Poon, J. F., and Pratt, D. A. (2018). Recent Insights on Hydrogen Atom Transfer in the Inhibition of Hydrocarbon Autoxidation. *Acc. Chem. Res.* **51**, 1996–2005.

5. Manfred-Weber, Markus-Weber, and Kleine-Boymann, M. (2012). Ullmann's Encyclopedia of Industrial Chemistry. 26.
6. Tomas, R. A. F., Bordado, J. C. M., and Gomes, J. F. P. (2013). p-Xylene Oxidation to Terephthalic Acid: A Literature Review Oriented toward Process Optimization and Development. *Chem. Rev.* 113, 7421–7469.
7. Vinogradov, M. G., Gachechiladze, G. G., Kereselidze, R. V., and Nikishin, G. I. (1969). Addition of Aldehydes to Unsaturated Compounds Induced by Autoxidation. *Russ. Chem. Bull.* 18, 276–281.
8. Chudasama, V., Fitzmaurice, R. J., and Caddick, S. (2010). Hydroacylation of Alpha, Beta-Unsaturated Esters via Aerobic C–H Activation. *Nat. Chem.* 2, 592–596.
9. Paul, S., and Guin, J. (2015). Dioxygen-Mediated Decarbonylative C–H Alkylation of Heteroaromatic Bases with Aldehydes. *Chem. Eur. J.* 21, 17618–17622.
10. Mukaiyama, T., and Yamada, T. (1995). Recent Advances in Aerobic Oxygenation. *Bull. Chem. Soc. Jpn.* 68, 17–35.
11. Yamada, T., Takai, T., Rhode, O., and Mukaiyama, T. (1991). Direct Epoxidation of Olefins Catalyzed by Nickel(II) Complexes with Molecular-Oxygen and Aldehydes. *Bull. Chem. Soc. Jpn.* 64, 2109–2117.
12. Yamada, T., Takai, T., Rhode, O., and Mukaiyama, T. (1991). Highly Efficient Method for Epoxidation of Olefins with Molecular-Oxygen and Aldehydes Catalyzed by Nickel(II) Complexes. *Chem. Lett.* 1–4.
13. Weinstein, A. B., and Stahl, S. S. (2014). Palladium Catalyzed Aryl C–H Amination with O₂ via In Situ Formation of Peroxide-Based Oxidant(s) from Dioxane. *Catal. Sci. Technol.* 4, 4301–4307.
14. Das, P., Saha, D., Saha, D., and Guin, J. (2016). Aerobic Direct C(sp²)–H Hydroxylation of 2-Arylpyridines by Palladium Catalysis Induced with Aldehyde Auto-Oxidation. *ACS Catal.* 6, 6050–6054.
15. Das, P., and Guin, J. (2018). Direct C(sp²)–H Hydroxylation of Arenes with Palladium(II)/Oxygen Using Sulfoximines as a Recyclable Directing Group. *Chemcatchem* 10, 2370–2373.
16. Bäckvall, J.-E., Awasthi, A. K., and Renko, Z. D. (1987). Biomimetic Aerobic 1,4-Oxidation of 1,3-Dienes Catalyzed by Cobalt Tetraphenylporphyrin-Hydroquinone-Palladium(II) - An Example of Triple Catalysis. *J. Am. Chem. Soc.* 109, 4750–4752.
17. Bäckvall, J.-E., Hopkins, R. B., Grennberg, H., Mader, M. M., and Awasthi, A. K. (1990) Multistep Electron-Transfer in Palladium-Catalyzed Aerobic Oxidations via a Metal Macrocycle–Quinone System. *J. Am. Chem. Soc.* 112, 5160–5166.
18. Morandi, B., Wickens, Z. K., and Grubbs, R. H. (2013). Practical and General Palladium-Catalyzed Synthesis of Ketones from Internal Olefins. *Angew. Chem. Int. Ed.* 52, 2944–2948.
19. Wendlandt, A. E., and Stahl, S. S. (2015). Quinone-Catalyzed Selective Oxidation of Organic Molecules. *Angew. Chem. Int. Ed.* 54, 14638–14658.
20. Stahl, S. S. (2004). Palladium Oxidase Catalysis: Selective Oxidation of Organic Chemicals by Direct Dioxygen-Coupled Turnover. *Angew. Chem. Int. Ed.* 43, 3400–3420.
21. Wang, D., Weinstein, A. B., White, P. B., and Stahl, S. S. (2018). Ligand-Promoted Palladium-Catalyzed Aerobic Oxidation Reactions. *Chem. Rev.* 118, 2636–2679.

22. ten Brink, G.-J., Arends, I., and Sheldon, R. A. (2000). Green, Catalytic Oxidation of Alcohols in Water. *Science* **287**, 1636–1639.

23. Ferreira, E. M., and Stoltz, B. M. (2001). The Palladium-Catalyzed Oxidative Kinetic Resolution of Secondary Alcohols with Molecular Oxygen. *J. Am. Chem. Soc.* **123**, 7725–7726.

24. Jensen, D. R., Pugsley, J. S., and Sigman, M. S. (2001). Palladium-Catalyzed Enantioselective Oxidations of Alcohols Using Molecular Oxygen. *J. Am. Chem. Soc.* **123**, 7475–7476.

25. Brice, J. L., Harang, J. E., Timokhin, V. I., Anastasi, N. R., and Stahl, S. S. (2005). Aerobic Oxidative Amination of Unactivated Alkenes Catalyzed by Palladium. *J. Am. Chem. Soc.* **127**, 2868–2869.

26. Passoni, L. C., Cruz, A. T., Buffon, R., and Schuchardt, U. (1997). Direct Selective Oxidation of Benzene to Phenol Using Molecular Oxygen in the Presence of Palladium and Heteropolyacids. *J. Mol. Catal. Chem.* **120**, 117–123.

27. Zhang, Y.-H., and Yu, J.-Q. (2009). Pd(II)-Catalyzed Hydroxylation of Arenes with 1 atm of O₂ or Air. *J. Am. Chem. Soc.* **131**, 14654–14655.

28. Boele, M. D. K., van Strijdonck, G. P. F., de Vries, A. H. M., Kamer, P. C. J., de Vries, J. G., and van Leeuwen, P. (2002). Selective Pd-Catalyzed Oxidative Coupling of Anilides with Olefins Through C–H Bond Activation at Room Temperature. *J. Am. Chem. Soc.* **124**, 1586–1587.

29. Dams, M., De Vos, D. E., Celen, S., and Jacobs, P. A. (2003). Toward Waste-Free Production of Heck Products with a Catalytic Palladium System under Oxygen. *Angew. Chem. Int. Ed.* **42**, 3512–3515.

30. Grimster, N. P., Gauntlett, C., Godfrey, C. R. A., and Gaunt, M. J. (2005). Palladium-Catalyzed Intermolecular Alkenylation of Indoles by Solvent-Controlled Regioselective C–H Functionalization. *Angew. Chem. Int. Ed.* **44**, 3125–3129.

31. Beck, E. M., Grimster, N. P., Hatley, R., and Gaunt, M. J. (2006). Mild Aerobic Oxidative Palladium(II) Catalyzed C–H Bond Functionalization: Regioselective and Switchable C–H Alkenylation and Annulation of Pyrroles. *J. Am. Chem. Soc.* **128**, 2528–2529.

32. Liu, G., Yin, G., and Wu, L. (2008). Palladium-Catalyzed Intermolecular Aerobic Oxidative Amination of Terminal Alkenes: Efficient Synthesis of Linear Allylamine Derivatives. *Angew. Chem. Int. Ed.* **47**, 4733–4736.

33. Reed, S. A., and White, M. C. (2008). Catalytic Intermolecular Linear Allylic C–H Amination via Heterobimetallic Catalysis. *J. Am. Chem. Soc.* **130**, 3316–3318.

34. Khusnutdinova, J. R., Qu, F., Zhang, Y., Rath, N. P., and Mirica, L. M. (2012). Formation of the Palladium(IV) Complex $[(\text{Me}_3\text{tacn})\text{Pd}^{\text{IV}}\text{Me}_3]^+$ through Aerobic Oxidation of $(\text{Me}_3\text{tacn})\text{Pd}^{\text{II}}\text{Me}_2$ ($\text{Me}_3\text{tacn} = \text{N},\text{N}',\text{N}''\text{-Trimethyl-1,4,7-triazacyclononane}$). *Organometallics* **31**, 4627–4630.

35. Khusnutdinova, J. R., Rath, N. P., and Mirica, L. M. (2012). The Aerobic Oxidation of a Pd(II) Dimethyl Complex Leads to Selective Ethane Elimination from a Pd(III) Intermediate. *J. Am. Chem. Soc.* **134**, 2414–2422.

36. Tang, F., Zhang, Y., Rath, N. P., and Mirica, L. M. (2012). Detection of Pd(III) and Pd(IV) Intermediates during the Aerobic Oxidative C–C Bond Formation from a Pd(II) Dimethyl Complex. *Organometallics* **31**, 6690–6696.

37. Liu, W. G., Sberegaaeva, A. V., Nielsen, R. J., Goddard, W. A., III, and Vedernikov, A. N. (2014). Mechanism of O₂ Activation and Methanol Production by (Di(2-

pyridyl)methanesulfonate)Pt(II)Me(OH_n)⁽²⁻ⁿ⁾⁻ Complex from Theory with Validation from Experiment. *J. Am. Chem. Soc.* **136**, 2335–2341.

38. Sberegaeva, A. V., Liu, W. G., Nielsen, R. J., Goddard, W. A., III, and Vedernikov, A. N. (2014). Mechanistic study of the oxidation of a methyl platinum(II) complex with O₂ in water: Pt(II)Me-to-Pt(IV)Me and Pt(II)Me-to-Pt(IV)Me₂ reactivity. *J. Am. Chem. Soc.* **136**, 4761–1768.

39. Hashimoto, T., Hirose, D., and Taniguchi, T. (2015). Catalytic Aerobic Oxidation of Arylhydrazides with Iron Phthalocyanine. *Adv. Synth. Catal.* **357**, 3346–3352.

40. Brand, J. P., González, D. F., Nicolai, S., and Waser, J. (2011). Benziodoxole-Based Hypervalent Iodine Reagents for Atom-Transfer Reactions. *Chem. Commun.* **47**, 102–115.

41. Singh, F. V., and Wirth, T. (2014). Comprehensive Organic Chemistry. *P. Knochel, 1Ind Ed.*, Elsevier 880–933.

42. Charpentier, J., Früh, N., and Togni, A. (2015). Electrophilic Trifluoromethylation by Use of Hypervalent Iodine Reagents. *Chem. Rev.* **115**, 650–682.

43. Yusubov, M. S., Yoshimura, A., and Zhdankin, V. V. (2016). Iodonium ylides in organic synthesis. *Arkivoc* **342**–374.

44. Yoshimura, A., Yusubov, M. S., and Zhdankin, V. V. (2016). Synthetic Applications of Pseudocyclic Hypervalent Iodine Compounds. *Org. Biomol. Chem.* **14**, 4771–4781.

45. Yoshimura, A., and Zhdankin, V. V. (2016). Advances in Synthetic Applications of Hypervalent Iodine Compounds. *Chem. Rev.* **116**, 3328–3435.

46. Sousa e Silva, F. C., Tierno, A. F., and Wengryniuk, S. E. (2017). Hypervalent Iodine Reagents in High Valent Transition Metal Chemistry. *Molecules* **22**, 780.

47. Recently, photochemically promoted one-electron reduction of I(III) species has been advanced as a strategy to generating iodanyl radicals in organic chemistry. See: Wang, X., and Studer, A. (2017). Iodine(III) Reagents in Radical Chemistry. *Acc. Chem. Res.* **50**, 1712–1724.

48. For examples of thermally promoted I–X homolysis, see reference 48–53. Magnus, P., Lacour, J., Evans, P. A., Roe, M. B., and Hulme, C. (1996). Hypervalent Iodine Chemistry: New Oxidation Reactions Using the Iodosylbenzene–Trimethylsilyl Azide Reagent Combination. Direct α- and β-Azido Functionalization of Triisopropylsilyl Enol Ethers. *J. Am. Chem. Soc.* **118**, 3406–3418.

49. Liu, X., Wang, Z., Cheng, X., and Li, C. (2012). Silver-Catalyzed Decarboxylative Alkyneylation of Aliphatic Carboxylic Acids in Aqueous Solution. *J. Am. Chem. Soc.* **134**, 14330–14333.

50. Kita, Y., Tohma, H., Hatanaka, K., Takada, T., Fujita, S., Mitoh, S., Sakurai, H., and Oka, S. (1994). Hypervalent Iodine-Induced Nucleophilic Substitution of para-Substituted Phenol Ethers. Generation of Cation Radicals as Reactive Intermediates. *J. Am. Chem. Soc.* **116**, 3684–3691.

51. Kantak, A. A., Potavathri, S., Barham, R. A., Romano, K. M., and DeBoef, B. (2011). Metal-Free Intermolecular Oxidative C–N Bond Formation via Tandem C–H and N–H Bond Functionalization. *J. Am. Chem. Soc.* **133**, 19960–19965.

52. Dohi, T., Ito, M., Morimoto, K., Iwata, M., and Kita, Y. (2008). Oxidative Cross-Coupling of Arenes Induced by Single-Electron Transfer Leading to Biaryls by Use of Organoiodine(III) Oxidants. *Angew. Chem. Int. Ed.* **47**, 1301–1304.

53. Dohi, T., Ito, M., Yamaoka, N., Morimoto, K., Fujioka, H., and Kita, Y. (2010). Unusual ipso Substitution of Diaryliodonium Bromides Initiated by a Single-Electron-Transfer Oxidizing Process. *Angew. Chem. Int. Ed.* **49**, 3334–3337.

54. For examples of photochemically promoted I–X homolysis, see reference 54–57. Le Vaillant, F., Courant, T., and Waser, J. (2015). Room-Temperature Decarboxylative Alkynylation of Carboxylic Acids Using Photoredox Catalysis and EBX Reagents. *Angew. Chem. Int. Ed.* **54**, 11200–11204.

55. Huang, H., Zhang, G., Gong, L., Zhang, S., and Chen, Y. (2014). Visible-Light-Induced Chemoselective Deboronative Alkynylation under Biomolecule-Compatible Conditions. *J. Am. Chem. Soc.* **136**, 2280–2283.

56. Zhou, Q.-Q., Guo, W., Ding, W., Wu, X., Chen, X., Lu, L.-Q., and Xiao, W.-J. (2015). Decarboxylative Alkynylation and Carbonylative Alkynylation of Carboxylic Acids Enabled by Visible-Light Photoredox Catalysis. *Angew. Chem. Int. Ed.* **54**, 11196–11199.

57. Tobisu, M., Furukawa, T., and Chatani, N. (2013). Visible Light-Mediated Direct Arylation of Arenes and Heteroarenes Using Diaryliodonium Salts in the Presence and Absence of a Photocatalyst. *Chem. Lett.* **42**, 1203–1205.

58. Maity, A., Hyun, S.-M., and Powers, D. C. (2017). Oxidase Catalysis via Aerobically Generated Hypervalent Iodine Intermediates. *Nat. Chem.* **10**, 200–204.

59. Maity, A., Hyun, S.-M., Wortman, A. K., and Powers, D. C. (2018). Oxidation Catalysis by an Aerobically Generated Dess–Martin Periodinane Analogue. *Angew. Chem. Int. Ed.* **57**, 7205–7209.

60. Miyamoto, K., Yamashita, J., Narita, S., Sakai, Y., Hirano, K., Saito, T., Wang, C., Ochiai, M., and Uchiyama, M. (2017). Iodoarene-Catalyzed Oxidative Transformations Using Molecular Oxygen. *Chem. Commun.* **53**, 9781–9784.

61. Dohi, T., and Kita, Y. (2009). Hypervalent Iodine Reagents as a New Entrance to Organocatalysts. *Chem. Commun.* 2073–2085.

62. Togo, H., Iinuma, M., and Moriyama, K. (2012). Simple and Practical Method for Preparation of [(Diacetoxy)iodo]arenes with Iodoarenes and *m*-Chloroperoxybenzoic Acid. *Synlett* **23**, 2663–2666.

63. Zhu, C., Liang, Y., Hong, X., Sun, H., Sun, W.-Y., Houk, K. N., and Shi, Z. (2015). Iodoarene-Catalyzed Stereospecific Intramolecular sp^3 C–H Amination: Reaction Development and Mechanistic Insights. *J. Am. Chem. Soc.* **137**, 7564–7567.

64. Yagyu, T., Takemoto, Y., Yoshimura, A., Zhdankin, V. V., and Saito, A. (2017). Iodine(III)-Catalyzed Formal [2+2+1] Cycloaddition Reaction for Metal-Free Construction of Oxazoles. *Org. Lett.* **19**, 2506–2509.

65. Qin, Y., Zhu, L., and Luo, S. (2017). Organocatalysis in Inert C–H Bond Functionalization. *Chem. Rev.* **117**, 9433–9520.

66. Clinton, N. A., Kenley, R. A., and Traylor, T. G. (1975). Acetaldehyde Autoxidation. I. Products of Termination. *J. Am. Chem. Soc.* **97**, 3746–3751.

67. Wentzel, B. B., Alsters, P. L., Feiters, M. C., and Nolte, R. J. M. (2004). Mechanistic Studies on the Mukaiyama Epoxidation. *J. Org. Chem.* **69**, 3453–3464.

68. Radical initiators are often used to promote autoxidation chemistry. In the absence of initiators, a variety of direct substrate / O_2 reactions have been invoked as the initial radical generating events. For discussion, see discussion in reference 1b.

69. For Russell termination mechanism, see reference 69–73. Blanchard, H. S. (1959). A Study of the Mechanism of Cumene Autoxidation. Mechanism of the Interaction of t-Peroxy Radicals. *J. Am. Chem. Soc.* **81**, 4548–4552.

70. McDowell, C. A., and Sifniades, S. (1963). Oxygen-18 Tracer Evidence for the Termination Mechanism in the Photochemical Oxidation of Acetaldehyde. *Can. J. Chem.* **41**, 300–307.

71. Ingold, K. U. (1969). Peroxy Radicals. *Acc. Chem. Res.* **2**, 1–9.

72. Howard, J. A., and Ingold, K. U. (1968). Self-Reaction of *sec*-Butylperoxy Radicals. Confirmation of the Russell Mechanism. *J. Am. Chem. Soc.* **90**, 1056–1058.

73. Zhang, P., Wang, W., Zhang, T., Chen, L., Du, Y., Li, C., and Lü, J. (2012). Theoretical Study on the Mechanism and Kinetics for the Self-Reaction of $C_2H_5O_2$ Radicals. *J. Phys. Chem. A* **116**, 4610–4620.

74. Sankar, M., Nowicka, E., Carter, E., Murphy, D. M., Knight, D. W., Bethell, D., and Hutchings, G. J. (2014). The Benzaldehyde Oxidation Paradox Explained by the Interception of Peroxy Radical by Benzyl Alcohol. *Nat. Commun.* **5**, 3332.

75. Jenkins, C. A. M., D. M., Rowlands, C. C., and Egerton, T. A. (1997). EPR Study of Spin-Trapped Free Radical Intermediates Formed in the Heterogeneously-Assisted Photodecomposition of Acetaldehyde. *J. Chem. Soc., Perkin Trans. 2* **2479**–2486.

76. Consistent with differences in solvent polarity (acetic acid versus dichloromethane) the measured coupling constants are slightly higher than those reported; see: Owenius, R., Engström, M., Lindgren, M., and Huber, M. (2001). Influence of Solvent Polarity and Hydrogen Bonding on the EPR Parameters of a Nitroxide Spin Label Studied by 9-GHz and 95-GHz EPR Spectroscopy and DFT Calculations. *J. Phys. Chem. A* **105**, 10967–10977.

77. Alberti, A., Carloni, P., Eberson, L., Greci, L., and Stipa, P. (1997). New Insights into N-*tert*-Butyl- α -phenylnitrone (PBN) as a Spin Trap. Part 2.1 The Reactivity of PBN and 5,5-Dimethyl-4,5-dihydropyrrole N-oxide (DMPO) toward N-Heteroaromatic Bases. *J. Chem. Soc., Perkin Trans. 2* **887**–892.

78. Yablonskii, O. P., Vinogradov, M. G., Kereselidze, R. V., and Nikishin, G. I. (1969). Mechanism of the Oxidation of Aldehydes by Oxygen. *Bull. Acad. Sci. USSR, Div. Chem. Sci.* **18**, 272–275.

79. Slagle, J., and Shine, H. (1959). Improved Yields in the Preparation of Diacetyl Peroxide. *J. Org. Chem.* **1959**, 24, 107.

80. Bawn, C. E. H., and Jolley, J. E. (1956). The Cobalt-Salt-Catalyzed Autoxidation of Benzaldehyde. *Proc. R. Soc., Lond., Ser. A* **237**, 297–312.

81. Jain, S. L., and Sain, B. (2003). An Unconventional Cobalt-Catalyzed Aerobic Oxidation of Tertiary Nitrogen Compounds to N-Oxides. *Angew. Chem. Int. Ed.* **42**, 1265–1267.

82. Hendriks, C. F., van Beek, H. C. A., and Heertjes, P. M. (1979). The Structure of Cobalt(II) Acetate and Cobalt(III) Acetate in Acetic Acid Solution. *Ind. Eng. Chem. Prod. Res. Dev.* **18**, 43–46.

83. Hendriks, C. F., van Beek, H. C. A., and Heertjes, P. M. (1979). Reactions of Some Peracids and Hydroperoxides with Cobalt(II) and Cobalt(III) Acetate in Acetic Acid Solution. *Ind. Eng. Chem. Prod. Res. Dev.* **18**, 38–43.

84. The induction period observed for oxidation of substituted aryl iodides is observed to vary, but when they are oxidized in a pairwise fashion, both begin displaying oxidation products at the same time.

85. In general, the best-fit lines of acquired substituent-dependent rates displayed small Y-intercepts. The Hammett plot of peracid oxidation rates fitted against σ^+ parameters displayed a Y-intercept of \sim –0.2; the data reported here is for a best-fit line that was forced through the origin. 4-Methoxyiodobenzene is not included on the peracid plot because the reaction product

was not the substituted diacetoxyiodobenzene observed for other substrates; the reaction product was not identified.

86. Howard, J. A., Ingold, K. U., and Symonds, M. (1968). Absolute Rate Constants for Hydrocarbon Oxidation. VIII. The Reactions of Cumylperoxy Radicals. *Can. J. Chem.* **46**, 1017–1022.
87. Nam, W., Kim, H. J., Kim, S. H., Ho, R. Y. N., and Valentine, J. S. (1996). Metal Complex-Catalyzed Epoxidation of Olefins by Dioxygen with Co-Oxidation of Aldehydes. A Mechanistic Study. *Inorg. Chem.* **35**, 1045–1049.
88. Murahashi, S., Oda, Y., and Naota, T. (1992). Iron- and Ruthenium-Catalyzed Oxidations of Alkanes with Molecular Oxygen in the Presence of Aldehydes and Acids. *J. Am. Chem. Soc.* **114**, 7913–7914.
89. Dell'Anna, M. M., Mastrorilli, P., and Nobile, C. F. (1998). Oxyfunctionalization of Hydrocarbons by In Situ Formed Peracid or by Metal Assisted Aerobic Oxidation. *J. Mol. Catal. A: Chemical* **130**, 65–71.
90. Muchalski, H., Levonyak, A. J., Xu, L., Ingold, K. U., and Porter, N. A. (2015). Competition H(D) Kinetic Isotope Effects in the Autoxidation of Hydrocarbons. *J. Am. Chem. Soc.* **137**, 94–97.
91. Along with 1-adamantanol, 2-adamantanone is observed in 5.3% yield.
92. I Iodosylbenzene exists as an extended -I-O-I- polymer. Computations reported by Zhdankin *et al.* describe the structure of monomeric iodosylbenzene as the zwitterionic structure that we present. See: Ivanov, A. S., Popov, I. A., Boldyrev, A. I., and Zhdankin, V. V. (2014). The I=X (X=O,N,C) Double Bond in Hypervalent Iodine Compounds: Is it Real? *Angew. Chem. Int. Ed.* **53**, 9617–9621.
93. Richter, H. W., Cherry, B. R., Zook, T. D., and Koser, G. F. (1997). Characterization of Species Present in Aqueous Solutions of [Hydroxy(mesyloxy)iodo]benzene and [Hydroxy(tosyloxy)iodo]benzene. *J. Am. Chem. Soc.* **119**, 9614–9623.
94. For simplicity, we have largely limited the presented pathways to those involving peracetic acid; related calculations using peroxide E and diacetyl peroxide H are presented in the Supporting Information.
95. Woods, K. W., and Beak, P. (1991). The Endocyclic Restriction Test: An Experimental Evaluation of the Geometry at Oxygen in the Transition Structure for Epoxidation of an Alkene by a Peroxy Acid. *J. Am. Chem. Soc.* **113**, 6281–6283.
96. Ramirez, F., and McKelvie, N. (1957). The Reaction of Trivalent Organophosphorus Compounds with Polyhalomethanes. *J. Am. Chem. Soc.* **79**, 5829–5830.
97. Walling, C., Basedow, O. H., and Savas, E. S. (1960). Some Extensions of the Reaction of Trivalent Phosphorus Derivatives with Alkoxy and Thiyl Radicals; a New Synthesis of Thioesters. *J. Am. Chem. Soc.* **82**, 2181–2184.
98. Walling, C., and Rabinowitz, R. (1959). The Reaction of Trialkyl Phosphites with Thiyl and Alkoxy Radicals. *J. Am. Chem. Soc.* **81**, 1243–1249.
99. Buckler, S. A. (1962). Autoxidation of Trialkylphosphines. *J. Am. Chem. Soc.* **84**, 3093–3097.
100. Bentruude, W. G. (1965). Autoxidation of Tertiary Phosphites. *Tetrahedron Lett.* **6**, 3543–3548.
101. Furimsky, E., and Howard, J. A. (1973). Absolute Rate Constants for the Reaction of tert-Butylperoxy Radicals with Trivalent Phosphorus Compounds. *J. Am. Chem. Soc.* **95**, 369–374.

102. Hwang, W.-S., and Yoke, J. T. (1980). Autoxidation of Ethyl Phosphinite, Phosphonite, and Phosphite Esters. *J. Org. Chem.* *45*, 2088–2091.

103. Potential one-electron oxidation of PhI with peracetic acid to generate a hydroxyiodinane and acetoxy radical **G** was computed to be uphill by 25.0 kcal/mol. Combined with the lack of detectable signals upon addition of PBN to the oxidation of PhI with peracetic acid, we have only considered pathways initiated by open-shell oxidants.

104. Alcock, N. W., Countryman, R. M., Esperås, S., and Sawyer, J. F. (1979). Secondary Bonding. Part 5. The Crystal and Molecular Structures of Phenyl iodine(III) Diacetate and Bis(dichloroacetate). *J. Chem. Soc., Dalton Trans. 0*, 854–860.

105. Li, G.-X., Morales-Rivera, C. A., Gao, F., Wang, Y., He, G., Liu, P., and Chen, G. (2017). A Unified Photoredox-Catalysis Strategy for C(sp³)-H Hydroxylation and Amidation Using Hypervalent Iodine. *Chem. Sci.* *8*, 7180–7185.

106. Li, G.-X., Morales-Rivera, C. A., Wang, Y., Gao, F., He, G., Liu, P., and Chen, G. (2016). Photoredox-Mediated Minisci C–H Alkylation of N-Heteroarenes Using Boronic Acids and Hypervalent Iodine. *Chem. Sci.* *7*, 6407–6412.

107. We have not been able to establish the chain length of autoxidation. Attempts to evaluate chain length by examining yield as a function of initiator loading are complicated by un-initiated background reaction.

108. Boisvert, L., Denney, M. C., Hanson, S. K., and Goldberg, K. I. (2009). Insertion of Molecular Oxygen into a Palladium(II) Methyl Bond: A Radical Chain Mechanism Involving Palladium(III) Intermediates. *J. Am. Chem. Soc.* *131*, 15802–15814.

109. Collins, K. D., and Glorius, F. (2013). A Robustness Screen for the Rapid Assessment of Chemical Reactions. *Nat. Chem.* *5*, 597–601.